

The influence of Langmuir turbulence on the scaling for the dissipation rate in the oceanic boundary layer

Article

Published Version

Teixeira, M. A. C. (2012) The influence of Langmuir turbulence on the scaling for the dissipation rate in the oceanic boundary layer. *Journal of Geophysical Research - Oceans*, 117 (C5). C05015. ISSN 0148-0227 doi:
<https://doi.org/10.1029/2011JC007235> Available at
<https://centaur.reading.ac.uk/29235/>

It is advisable to refer to the publisher's version if you intend to cite from the work. See [Guidance on citing](#).

Published version at: <http://dx.doi.org/10.1029/2011JC007235>

To link to this article DOI: <http://dx.doi.org/10.1029/2011JC007235>

Publisher: American Geophysical Union

All outputs in CentAUR are protected by Intellectual Property Rights law, including copyright law. Copyright and IPR is retained by the creators or other copyright holders. Terms and conditions for use of this material are defined in the [End User Agreement](#).

www.reading.ac.uk/centaur

CentAUR

Central Archive at the University of Reading

Reading's research outputs online

The influence of Langmuir turbulence on the scaling for the dissipation rate in the oceanic boundary layer

Miguel A. C. Teixeira¹

Received 22 April 2011; revised 16 March 2012; accepted 27 March 2012; published 9 May 2012.

[1] A model for estimating the turbulent kinetic energy dissipation rate in the oceanic boundary layer, based on insights from rapid-distortion theory, is presented and tested. This model provides a possible explanation for the very high dissipation levels found by numerous authors near the surface. It is conceived that turbulence, injected into the water by breaking waves, is subsequently amplified due to its distortion by the mean shear of the wind-induced current and straining by the Stokes drift of surface waves. The partition of the turbulent shear stress into a shear-induced part and a wave-induced part is taken into account. In this picture, dissipation enhancement results from the same mechanism responsible for Langmuir circulations. Apart from a dimensionless depth and an eddy turn-over time, the dimensionless dissipation rate depends on the wave slope and wave age, which may be encapsulated in the turbulent Langmuir number La_t . For large La_t , or any La_t but large depth, the dissipation rate tends to the usual surface layer scaling, whereas when La_t is small, it is strongly enhanced near the surface, growing asymptotically as $\varepsilon \propto La_t^{-2}$ when $La_t \rightarrow 0$. Results from this model are compared with observations from the WAVES and SWADE data sets, assuming that this is the dominant dissipation mechanism acting in the ocean surface layer and statistical measures of the corresponding fit indicate a substantial improvement over previous theoretical models. Comparisons are also carried out against more recent measurements, showing good order-of-magnitude agreement, even when shallow-water effects are important.

Citation: Teixeira, M. A. C. (2012), The influence of Langmuir turbulence on the scaling for the dissipation rate in the oceanic boundary layer, *J. Geophys. Res.*, 117, C05015, doi:10.1029/2011JC007235.

1. Introduction

[2] A problem in oceanography that has generated some controversy in recent years is the scaling for the dissipation rate of turbulent kinetic energy (TKE) in the oceanic boundary layer (OBL). This quantity influences gas transfer across the air-water interface (by controlling surface renewal), and is also important for small-scale mixing in the upper ocean [Teixeira and Belcher, 2000]. It has become clear that, in this and other respects, the OBL differs markedly from the atmospheric boundary layer (ABL), and the scalings which are applicable to one case are not transposable to the other. It is widely recognized that these differences are essentially due to the existence of surface waves, however the exact mechanisms through which the waves give rise to these differences have not been totally clarified.

[3] In the ABL, the mean velocity profile in the surface layer typically follows a logarithmic variation, and consistently in the TKE budget the shear production term is

approximately balanced by dissipation, with the rate of dissipation of TKE scaling like $\varepsilon = u_*^3/(\kappa|z|)$. In the OBL, however, the dissipation rate is often observed to exceed this estimate by orders of magnitude, and various models have been proposed to explain this phenomenon. Initial attempts toward that aim [e.g., Drennan *et al.*, 1992] merely noted the similarity between the power laws observed near the surface for the dissipation rate as a function of depth and the corresponding behavior in grid-stirred water tanks ($\varepsilon \propto |z|^{-4}$).

[4] More elaborate scalings have been developed, considering possible balances in the equations of motion. Craig and Banner [1994], for example, assumed that turbulent transport balances dissipation in the near-surface TKE budget, leading to a dependence of the type $\varepsilon \propto |z|^{-3.4}$. However, their model is extremely sensitive to the value of the water-side roughness length z_0 . Anis and Moum [1995], on the other hand, considered two wave-turbulence interaction mechanisms: one of them relying on the transport of TKE by the orbital wave motions, and the other relying on the wave-induced shear stress existing in a rotational wavefield. Both mechanisms lead to an exponential variation of ε with $|z|$. However, analysis of the dissipation data of Terray *et al.* [1996], Drennan *et al.* [1996] and Gerbi *et al.* [2009], in addition to those of Anis and Moum [1995] themselves, show that the variation of ε with depth is much faster than

¹CGUL, IDL, University of Lisbon, Lisbon, Portugal.

Corresponding author: M. A. C. Teixeira, CGUL, IDL, University of Lisbon, Edifício C8, Campo Grande, P-1749-016 Lisbon, Portugal. (mateixeira@fc.ul.pt)

Copyright 2012 by the American Geophysical Union.
0148-0227/12/2011JC007235

exponential. On the other hand, the parameters used in both models proposed by *Anis and Moum* [1995] (the correlation coefficient between the wave and turbulence velocity fluctuations and the phase angle by which the wave velocity components are out of quadrature) are hard to estimate independently. Finally, *Terray et al.* [1996] used dimensional analysis and observations to establish the dependence of the normalized dissipation rate on a number of dimensionless parameters. Invoking some approximations, they reduced the number of these parameters to one, obtaining a scaling for which $\varepsilon \propto |z|^{-2}$.

[5] While there is considerable disagreement about the functional form for the dependence of the dissipation rate with depth, all the authors cited above agree that one aspect of the waves which is relevant to this problem is wave breaking. Underlying most of the mechanisms described above is the idea that the dissipation rate enhancement near the surface is directly caused by the injection of turbulence into the water by breaking waves. *Teixeira* [2011b] proposed a complementary mechanism, where turbulence, most probably produced by wave breaking, but which might also be generated by any other process (e.g., instability of a wind-driven shear current), is distorted and amplified by the joint action of a mean Eulerian current and the Stokes drift of irrotational surface waves. In this mechanism, which assumes that the dissipation rate is balanced at equilibrium by production of TKE by mean shear and by Stokes drift straining, the primary reason for dissipation enhancement is the same instability mechanism that gives rise to Langmuir circulations, which strongly amplifies the shear stress near the surface. *Teixeira* [2011b] made preliminary comparisons of results from his calculations to data from *Agrawal et al.* [1992], *Terray et al.* [1996] and *Drennan et al.* [1996], finding order-of-magnitude agreement. However, more systematic tests are required to evaluate the usefulness of those calculations. Additionally, one problematic assumption made by *Teixeira* [2011b] is that the profile of the wind-induced water current remains logarithmic and with the same friction velocity as when there is no Craik-Leibovich instability. This is in contradiction with the findings of, for example, *McWilliams et al.* [1997], *Li et al.* [2005] and *Polton and Belcher* [2007], who show that the shear in this current weakens considerably in the presence of Langmuir circulations.

[6] The present study uses observations from various sources (including the field campaigns WAVES and SWADE) to show that the mechanism for the enhancement of the dissipation rate proposed by *Teixeira* [2011b] can provide a better estimate of this quantity than a number of previous models, including those of *Craig and Banner* [1994] and of *Terray et al.* [1996]. The assumption of a logarithmic water current profile is, however, corrected, assuming instead that the shear stress near the surface is partitioned between a shear-induced and a wave-induced part (as noted in *Teixeira* [2011a]), with the former becoming smaller as the turbulent Langmuir number La_t decreases.

[7] The new dissipation model is tested in the absence of any other dissipation enhancement mechanisms, through the calculation of statistics of its fit to the WAVES and SWADE data sets. While this approach is rather radical, it is adopted here for simplicity. It is not claimed that this is the only dissipation enhancement mechanism acting in the OBL.

However, if the present model shows an improved performance over existing models, as turns out to be the case, this suggests that the corresponding mechanism may be dominant over those previously proposed. The new model is also shown to avoid a number of inconsistencies displayed by previous models with other data sets, namely the need to recalibrate the constant in the wave energy input parameter (which is not a key parameter in the dissipation scaling presented here), and an unsatisfactory performance in shallow-water conditions.

[8] This paper is organized as follows: in section 2, the model for the dissipation rate is presented. Section 3 contains the results, which include tests to the model using data from the WAVES and SWADE campaigns, and comparisons with more recent observations. Finally, in section 4, an overview of the main findings is presented.

2. Theoretical Model

[9] *Teixeira and Belcher* [2010] and *Teixeira* [2011a] used rapid-distortion theory (RDT) to investigate the characteristics of turbulence in the OBL. RDT is a highly idealized theory, where the equations of motion are linearized with respect to the turbulence. Nevertheless, when taking into account distortion of the turbulence by two external forcings—the mean shear associated with an Eulerian mean current driven by the wind stress and the gradient of the mean Lagrangian transport associated with the Stokes drift of surface waves—it was possible to produce turbulent flow structures, like streaks and streamwise vortices, which are observed in the OBL. Furthermore, the turbulence anisotropy and elongation were shown to be qualitatively, and even quantitatively concerning some aspects, in agreement with LES data of fully nonlinear OBL flows.

[10] One consequence of *Teixeira's* [2011a] calculations was the identification of a mechanism for the amplification of the turbulent shear stress through the same instability that leads to the initial exponential growth of Langmuir circulations. This led to the derivation by *Teixeira* [2011b] of an estimate for the TKE dissipation rate, using standard assumptions of RDT, namely that turbulence in equilibrium (where TKE production balances dissipation) has roughly similar characteristics to turbulence subjected to external forcings (as assumed in RDT) over a time of the order one eddy turn-over time. The reasoning of *Teixeira* [2011a, 2011b] relevant to TKE dissipation will be briefly recalled next.

[11] The inviscid and non-rotating equations of motion linearized with respect to the turbulent quantities and containing a ‘vortex force’ term [cf. *Leibovich*, 1983; *McWilliams et al.*, 1997; *Teixeira*, 2011a] are considered. Combining these equations, and subject to the above assumptions, *Teixeira* [2011a] found that the turbulent shear stress satisfies:

$$\begin{aligned} \frac{d^2 \overline{uw}}{dt^2} - 4 \frac{dU}{dz} \frac{dU_S}{dz} \overline{uw} = & -\frac{1}{\rho} \frac{d}{dt} \left(\overline{w \frac{\partial p}{\partial x}} + \overline{u \frac{\partial p}{\partial z}} \right) \\ & - \frac{2}{\rho} \left(\frac{dU}{dz} \overline{w \frac{\partial p}{\partial z}} + \frac{dU_S}{dz} \overline{u \frac{\partial p}{\partial x}} \right), \end{aligned} \quad (1)$$

where U is the mean velocity (associated with an Eulerian mean current), U_S is the Stokes drift velocity (associated with the Lagrangian mean transport induced by surface waves),

(u, v, w) is the turbulent velocity (including Langmuir cells or any other large-scale coherent structures), p is the turbulent pressure, ρ is the density (assumed to be constant), and the overbar denotes ensemble averaging. In this equation, it was assumed that both dU/dz and dU_S/dz are in the x direction (a situation consistent with the existence of wind waves, when the wind stress and the Stokes drift of surface waves are roughly aligned), and that U and U_S only depend on z . Additionally, it was assumed that the turbulence statistics (e.g., second-order correlations of turbulent quantities) also only depend on z . This is consistent with a horizontally statistically homogeneous situation.

[12] If p can be considered of secondary importance in the evolution of the shear stress, then it follows that:

$$\frac{d^2 \overline{uw}}{dt^2} - 4 \frac{dU}{dz} \frac{dU_S}{dz} \overline{uw} = 0. \quad (2)$$

This neglect of the pressure is a common assumption in ‘parcel methods’ used to investigate numerous geophysical instabilities [cf. *Holton*, 2004] and is adopted here for mathematical convenience. Its approximate validity in the present context was shown by *Teixeira* [2011a].

[13] When $(dU/dz)(dU_S/dz) > 0$ (which is typically satisfied for wind waves, because the surface wind stress and the Stokes drift of the waves are roughly in the same direction), (2) has exponentially growing or decaying solutions. For dissipation enhancement, only the exponentially growing solution is relevant, so the shear stress evolves in time, at least initially, approximately according to

$$\overline{uw} = \overline{uw}(t=0) \exp \left[2 \left(\frac{dU}{dz} \frac{dU_S}{dz} \right)^{1/2} t \right]. \quad (3)$$

The growth rate of the shear stress is in this case similar to that derived by Craik and Leibovich [see *Leibovich*, 1983] for Langmuir circulations in a neutrally stratified ocean, which is not surprising since the physical mechanism at work is the same. The shear stress for turbulence in equilibrium is, according to RDT, approximately described by (3) with $t = T_L$ where T_L is the eddy turn-over time.

[14] The initial state of the turbulence assumed in the RDT calculations is that of turbulence embedded in a mean shear flow similar to that which exists in a stationary ABL, with the difference that the effect of the Stokes drift of surface waves is included (see details in *Teixeira* [2011b]). Therefore, the shear stress is assumed to be initially constant,

$$\overline{uw}(t=0) = -u_*^2, \quad (4)$$

where u_* is the friction velocity in the water, as derived from viscous coupling between the ABL and the OBL.

[15] The Stokes drift is assumed to be that corresponding to an irrotational monochromatic surface wave (which represents the peak of the surface wave spectrum),

$$\frac{dU_S}{dz} = 2(a_w k_w)^2 \sigma_w e^{-2k_w |z|}, \quad (5)$$

where a_w , k_w and σ_w are, respectively, the amplitude, wave number and angular frequency of the wave. This is done for simplicity, since the use of a full wave spectrum would

introduce additional input parameters into the model. In fact, except very close to the surface, the contribution of surface waves to the Stokes drift gradient comes mainly from the spectral peak [*Teixeira*, 2011b].

[16] Due to the presence of surface waves, the mean shear stress \overline{uw} is partitioned between a shear-induced and a wave-induced part. *Teixeira* [2011a, equation (19)] proposed a parameterization for this partition based on the linearized equation for \overline{uw} . In this equation, the mechanical production terms due to mean shear and the Stokes drift strain are, respectively, $\overline{w^2} dU/dz$ and $\overline{u^2} dU_S/dz$, where $\overline{u^2}$ and $\overline{w^2}$ are the streamwise and vertical velocity variances. If one accepts that \overline{uw} is primarily shaped by these mechanical production terms, then it seems reasonable to assume that its shear-induced part is proportional to the fraction of the mechanical production terms corresponding to shear production [cf. *Teixeira*, 2011a, equation (30)], yielding:

$$(\overline{uw})_s = - \frac{u_*^2}{1 + \frac{\overline{u^2}}{\overline{w^2}} \frac{dU_S/dz}{dU/dz}}. \quad (6)$$

[17] It is fairly obvious that the ratio $(dU_S/dz)/(dU/dz)$ is proportional to $La_t^{-2} = U_S(z=0)/u_*$ [see *Teixeira*, 2011a, equation (31)], and it should also contain the exponential vertical dependence of the Stokes drift of surface waves. On the other hand, the ratio $\overline{u^2}/\overline{w^2}$ is *a priori* unknown, but it should tend to infinity as $z \rightarrow 0$, while $(dU/dz)^{-1}$ should tend to zero as $z \rightarrow 0$, because it is proportional to the eddy-viscosity, which, in the surface layer shows a similar dependence. Assuming that the z dependence of $\overline{u^2}/\overline{w^2}$ and of $(dU/dz)^{-1}$ cancels, a parameterization for the part of the shear stress associated with mean shear takes the form:

$$(\overline{uw})_s = - \frac{u_*^2}{1 + \gamma La_t^{-2} e^{-2k_w |z|}}, \quad (7)$$

where γ is an adjustable constant. In addition, the usual surface layer turbulence closure is adopted here only for $(\overline{uw})_s$ (as makes sense physically):

$$(\overline{uw})_s = -K_m \frac{dU}{dz}, \quad (8)$$

where, however, $K_m = \kappa u_* z$ is defined using the ‘total’ friction velocity u_* , as usual. Then, using (7) and (8), it turns out that the mean shear rate can be written:

$$\frac{dU}{dz} = \frac{u_*}{\kappa |z|} \frac{1}{1 + \gamma La_t^{-2} e^{-2k_w |z|}}, \quad (9)$$

where κ is Von Kármán’s constant. Equation (9) expresses the fact that the velocity profile is no longer logarithmic, and the mean shear is reduced as La_t decreases. This only happens near the surface, over the depth range where the Stokes drift is important. Note that, by (7) and (9), this corresponds to the definition of a surrogate friction velocity associated only with mean shear,

$$u_{*s} = - \frac{(\overline{uw})_s(z=0)}{u_*} = \frac{u_*}{1 + \gamma La_t^{-2}}, \quad (10)$$

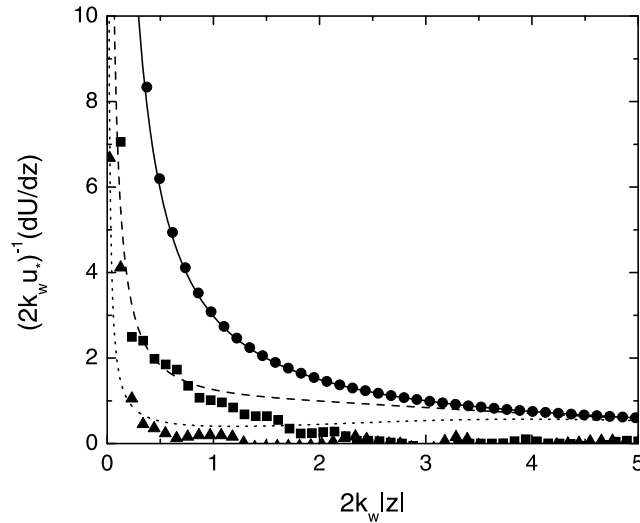


Figure 1. Normalized shear rate as a function of normalized depth for the mean velocity profiles presented in *Li et al.* [2005, Figure 2e] (symbols) against predictions of the same quantity from (9) (lines). Circles and solid line: $La_t = 10$, squares and dashed line: $La_t = 0.73$, triangles and dotted line: $La_t = 0.34$.

which becomes a progressively smaller fraction of u_* as La_t decreases. The need to use a reduced friction velocity in the presence of Langmuir turbulence was noted by *Teixeira and Belcher* [2010]. In order to calibrate the constant γ in (7), the mean velocity profiles presented in *Li et al.* [2005, Figure 2e] for various La_t will be used.

[18] Figure 1 shows dU/dz as derived from the data of *Li et al.* [2005] after some smoothing (symbols), against predictions from (9) with $\gamma = 2$ (lines) for $La_t = 10$, $La_t = 0.73$ and $La_t = 0.34$. It can be seen that for $La_t = 10$ (which is effectively equivalent to $La_t = \infty$) the agreement with (9) is excellent, showing that the mean velocity profile is logarithmic, despite the fact that the shear stress is not constant [see *Li et al.*, 2005, Figure 2d]. For $La_t = 0.73$ and $La_t = 0.34$, the shear rate near the surface is well approximated by (9), although further below it is overestimated. This may be attributed to vertical mixing caused by the turbulence, a higher-order effect neglected in the present model. Nevertheless, what is important for the present calculations is the ability to reproduce correctly the order of magnitude of the shear rate near the surface, where this quantity is highest, and this is achieved by (9) with $\gamma = 2$.

[19] It is assumed that, throughout the distortion described by (3), both the mean velocity and the Stokes drift retain their initial forms (9) and (5). Especially in the case of the mean velocity, this is not strictly true, because the vertical mixing induced by the change in the turbulence characteristics as the distortion progresses tends to weaken the mean shear, as noted above [*Teixeira and Belcher*, 2010]. However, this might be an effect of secondary importance, because it occurs at depths where the shear rate is lower, and during the course of the amplification of \overline{uw} that causes the enhancement of ε . So it can be argued that this amplification must be influenced by the initial state of the shear rate, still unaffected by this mixing, to some degree.

[20] The mean velocity profile (9) could also be destroyed by wave breaking, but this effect is more intermittent and localized than that of the wind stress that forces the current [*Sullivan et al.*, 2004].

[21] Finally, it is assumed that, at equilibrium, turbulence production by the shear and Stokes drift straining balances dissipation in the TKE budget, that is:

$$\varepsilon = -\overline{uw} \left(\frac{dU}{dz} + \frac{dU_S}{dz} \right). \quad (11)$$

This balance is questioned by some authors [e.g., *Craig and Banner*, 1994; *Noh et al.*, 2004], who argue instead for a balance between dissipation and turbulent transport, associated with the injection of turbulence into the water by breaking waves. However, there is no conclusive evidence to support that hypothesis beyond doubt, since existing wave breaking representations in LES (which are the only practical means of analyzing the TKE budget), are questionable. The argument of *Teixeira* [2011b] to support (11) is based on the idea that wave breaking is highly intermittent [*Sullivan et al.*, 2004, 2007], and that the balance expressed by (11) could be reached after the shear stress has been amplified considerably by the instability mechanism described by (3). The dominant contributions to the dissipation rate should occur at this stage. Additional support for (11) is given by the TKE budgets presented in the LES studies of *Polton and Belcher* [2007], *Grant and Belcher* [2009], and *Kukulka et al.* [2010], which show a dominant balance between the sum of the mechanical production terms and dissipation over the sum of the turbulent flux terms, particularly near the surface, although these studies neglected wave breaking. Other studies including the effect of wave breaking [*Noh et al.*, 2004; *Sullivan et al.*, 2007] parameterized this effect in a way whose physical basis is not as solid as that of the effect of the Stokes drift, so their results are not wholly reliable. Additionally, these studies did not explicitly analyze the TKE budget. For those reasons, the processes that balance dissipation in the OBL cannot be considered sufficiently well-known, and (11) is adopted here as a working hypothesis.

[22] Given these cautions, and taking into account (3) evaluated at $t = T_L$, and also (4) and (11), it follows that at equilibrium

$$\varepsilon = u_*^2 \left(\frac{dU}{dz} + \frac{dU_S}{dz} \right) \exp \left[2 \left(\frac{dU}{dz} \frac{dU_S}{dz} \right)^{1/2} T_L \right]. \quad (12)$$

A key quantity in (12), but one of the most difficult to estimate from standard data, given that it depends on characteristics of the turbulence in the OBL, is T_L . *Teixeira* [2011b] estimated this quantity as $T_L \approx l/u_*$, where l is a representative length scale of the turbulence near the surface. Since the most likely source for the turbulence that causes dissipation enhancement is wave breaking, the length scale used for estimating T_L should be related to the characteristics of the dominant waves. For that reason, in the present study it will be assumed, as in *Teixeira* [2011b], that

$$T_L = c \frac{k_w^{-1}}{u_*}, \quad (13)$$

where c is a dimensionless constant. This implies that l is proportional to the wavelength of the dominant waves. The only other wave length scale available apart from k_w^{-1} is the wave amplitude a_w , but tests (not shown) revealed that this choice would degrade the performance of the model.

[23] Like *Agrawal et al.* [1992] and *Melville* [1996], *Teixeira* [2011b] provided an expression for the dissipation rate normalized using u_* and z as a function of depth normalized by u_* and g (the acceleration of gravity). However, especially since the studies of *Terray et al.* [1996] and *Drennan et al.* [1996], it became more usual to scale the dissipation rate using the wave significant height H_s and the energy flux into the waves F . The latter quantity was initially defined by *Terray et al.* [1996] in two different ways depending on the wave age, but more recently the following unique definition has become more popular [*Burchard*, 2001; *Feddersen et al.*, 2007; *Gerbi et al.*, 2009]:

$$F = \alpha u_*^3, \quad (14)$$

where α is a dimensionless constant, generally assumed to be $\alpha = 100$. Taking into account (9), (5) and (13), and normalizing z using H_s and ε using H_s and F , (12) may be shown to be equivalent to

$$\frac{\varepsilon H_s}{F} = \frac{1}{\alpha} \left[\frac{1}{\kappa(|z|/H_s)} \phi(z) + \frac{1}{4} (k_w H_s)^3 \left(\frac{c_w}{u_*} \right) e^{-2(k_w H_s)(\frac{|z|}{H_s})} \right] \times \exp \left\{ c \left[\left(\frac{c_w}{u_*} \right) \frac{1}{\kappa(|z|/H_s)} \phi(z) \right]^{1/2} (k_w H_s)^{1/2} e^{-(k_w H_s)(\frac{|z|}{H_s})} \right\}, \quad (15)$$

where

$$\phi(z) = \frac{1}{1 + 2La_t^{-2} e^{-2k_w|z|}} = \frac{1}{1 + \frac{1}{4} (k_w H_s)^2 \left(\frac{c_w}{u_*} \right)^2 e^{-2(k_w H_s)|z|/H_s}}, \quad (16)$$

and where the linear dispersion relation of deep-water surface gravity waves, $\sigma_w^2 = gk_w$, and the definition of phase velocity, $c_w = \sigma_w/k_w$, have been used. In (15), the significant wave height was related to the monochromatic wave amplitude through $H_s = 2\sqrt{2}a_w$. This results from noting that $H_s = 4(\overline{\zeta^2})^{1/2}$, where $(\overline{\zeta^2})^{1/2}$ is the root-mean square surface elevation [see *Csanady*, 2004] and that, for a monochromatic wave $(\overline{\zeta^2})^{1/2} = a_w/\sqrt{2}$. In (16), the definition of the turbulent Langmuir number $La_t = [(a_w k_w)^2 c_w / u_*]^{-1/2}$ was also used.

[24] Apart from $|z|/H_s$ and c , (15) shows that the normalized dissipation rate depends on $k_w H_s$ and c_w/u_* , which are parameters related to the wave slope and wave age, respectively, and equivalent to those found by *Teixeira* [2011b].

[25] If the definition of the turbulent Langmuir number, La_b , is used, and the length scale used to normalize both ε and z is k_w instead of H_s , then (15) becomes:

$$\frac{\varepsilon}{k_w F} = \frac{1}{\alpha} \left[\frac{1}{\kappa(k_w|z|)} \phi(z) + 2La_t^{-2} e^{-2k_w|z|} \right] \times \exp \left\{ 2cLa_t^{-1} \left[\frac{2}{\kappa(k_w|z|)} \phi(z) \right]^{1/2} e^{-k_w|z|} \right\}. \quad (17)$$

Normalizing ε using z instead of k_w , (17) can also be written:

$$\frac{\varepsilon \kappa|z|}{u_*^3} = \left[\phi(z) + 2\kappa La_t^{-2} (k_w|z|) e^{-2k_w|z|} \right] \times \exp \left\{ 2cLa_t^{-1} \left[\frac{2}{\kappa(k_w|z|)} \phi(z) \right]^{1/2} e^{-k_w|z|} \right\}. \quad (18)$$

Note that (18) only differs from *Teixeira* [2011b, equation (11)] by the presence of function $\phi(z)$ (which accounts for the partition of the shear stress into shear-induced and wave-induced parts), and reduces to that equation when $\phi(z) = 1$.

[26] These forms, where the depth scales on k_w^{-1} , emphasize the connection between dissipation enhancement and Langmuir turbulence, since apart from depth and c the normalized dissipation rate only depends on La_t (note that, from (16), $\phi(z)$ also only depends on La_t and $k_w|z|$). For $La_t \gg 1$ or large depths $k_w|z| \gg 1$, $\varepsilon/(k_w F)$ or $\varepsilon \kappa|z|/u_*^3$ reduce to the ABL surface layer scaling form, in agreement with the data of *Agrawal et al.* [1992]. For low La_t , on the other hand, the normalized dissipation rate is strongly enhanced relative to the usual surface layer scaling. In fact, it can be shown that, in the limit $La_t \rightarrow 0$, the dissipation rate becomes proportional to La_t^{-2} , because the dependence on La_t of the main exponential in (17) or (18) cancels out. This result is consistent with the scaling inferred for ε by *Grant and Belcher* [2009] at low La_t (without the present theoretical basis).

[27] Incidentally, (17), where $\varepsilon/(k_w F)$ is presented as a function of $k_w|z|$, has a generically similar form to a scaling suggested by *Drennan et al.* [1996] as an alternative to that of *Terray et al.* [1996]. Note that, while in (15) and (17) ε is normalized by F , α appears on the right hand side in both equations. This means that the value of α is immaterial for the scaling presented here, as is clearly confirmed by (18), where α does not appear. Therefore, F is not a key parameter in the present model.

[28] All of the above calculations have been carried out assuming that the surface waves are in deep water. In the more general case of arbitrary water depth h , the Stokes drift profile for a monochromatic surface water wave is instead given by

$$\frac{dU_S}{dz} = (a_w k_w)^2 \sigma_w \frac{\sinh[2k_w(h - |z|)]}{\sinh^2(k_w h)}. \quad (19)$$

Then it can be shown that, for example, (15) becomes:

$$\frac{\varepsilon H_s}{F} = \frac{1}{\alpha} \left\{ \frac{1}{\kappa(|z|/H_s)} \phi(z) + \frac{1}{8} (k_w H_s)^3 \left(\frac{c_w}{u_*} \right) \times \frac{\sinh[2k_w h - 2(k_w H_s)(|z|/H_s)]}{\sinh^2(k_w h)} \right\} \times \exp \left\{ c \left[\left(\frac{c_w}{u_*} \right) \frac{1}{2\kappa(|z|/H_s)} \phi(z) \right]^{1/2} (k_w H_s)^{1/2} \times \frac{\sinh^{1/2}[2k_w h - 2(k_w H_s)(|z|/H_s)]}{\sinh(k_w h)} \right\}, \quad (20)$$

where $\phi(z)$ must also have a modified form due to the dependence of the shear-induced part of the shear stress on dU_s/dz (see (6)):

$$\phi(z) = \frac{1}{1 + La_t^{-2} \frac{\sinh(2k_w h - 2k_w |z|)}{\sinh^2(k_w h)}} = \frac{1}{1 + \frac{1}{8} (k_w H_s)^2 \left(\frac{c_w}{u_*} \right) \frac{\sinh[2k_w h - 2(k_w H_s)|z|/H_s]}{\sinh^2(k_w h)}}. \quad (21)$$

These last equations should be used in cases where shallow-water effects are important.

3. Results

[29] Results from the model described above will be compared next with field data from various sources and results from previous models. In the data analysis that follows, three measures of the performance of the models for the dissipation rate will be used. The first of these measures is the correlation coefficient, which is defined as:

$$R = \frac{\sum_{i=1}^n (x_i - \bar{x})(y_i - \bar{y})}{\sqrt{\sum_{i=1}^n (x_i - \bar{x})^2} \sqrt{\sum_{i=1}^n (y_i - \bar{y})^2}}, \quad (22)$$

where x_i is a generic observation, y_i is a generic prediction, n is the number of observations and \bar{x} and \bar{y} are the averages of x_i and y_i , respectively. Secondly, the goodness of fit will be evaluated through a linear regression:

$$y = \alpha + \beta x, \quad (23)$$

where

$$\beta = \frac{\sum_{i=1}^n (x_i - \bar{x})(y_i - \bar{y})}{\sum_{i=1}^n (x_i - \bar{x})^2}, \quad \alpha = \bar{y} - \beta \bar{x}. \quad (24)$$

Thirdly and finally, the root-mean square error (RMSE) will be calculated:

$$\text{RMSE} = \sqrt{\frac{\sum_{i=1}^n (y_i - x_i)^2}{n}}. \quad (25)$$

[30] Since most recent studies about TKE dissipation in the OBL focus on $\varepsilon' = \varepsilon H_s / F$, (15) will be used to obtain theoretical values of the dissipation rate. As TKE dissipation is a highly intermittent process, when plotted in graphs with linear axes ε' tends to have apparent outliers, which artificially increase the correlation coefficient. For that reason the quantity that will be considered in the analysis that follows is $\log(\varepsilon')$, which makes the data distribution more homogeneous. Consider a relationship between the predicted and the observed values of ε' , ε'_p and ε'_o , respectively:

$$\varepsilon'_p = a \varepsilon_o'^b, \quad (26)$$

where a and b are constant coefficients. Taking the logarithm of (26), one obtains

$$\log(\varepsilon'_p) = \log a + b \log(\varepsilon'_o). \quad (27)$$

In (27), if $\log(\varepsilon'_o)$ and $\log(\varepsilon'_p)$ correspond to x and y , respectively, clearly $\log a$ and b correspond to the coefficients α and β in (23). If the prediction of the theoretical models was perfect, this would correspond to $R = 1$, $a = 1$, $b = 1$ and $\text{RMSE} = 0$. R decreases and RMSE increases as the predictions of $\log(\varepsilon')$ depart from the corresponding observations. If b differs from 1, this means that the relationship between ε'_p and ε'_o is not linear. If, on the other hand, b is near 1 but $a \neq 1$, the predictions either tend to underestimate (if $a < 1$) or overestimate the observations (if $a > 1$).

3.1. Comparisons With the WAVES and SWADE Data Sets

[31] The WAVES [Terray *et al.*, 1996] and SWADE [Drennan *et al.*, 1996] data sets are first used to calibrate the model constant c in (13). Using values of the dissipation rate from these two data sets, derived from both the horizontal and the vertical velocity spectra, it could be found that the RMSE is minimized for $c = 0.64$. From (13), this means that the assumed length scale for the turbulence that determines the eddy turn-over time is a relatively small fraction of the wavelength of the dominant surface waves (about 10%). This makes sense physically, since wave breaking, which presumably generates this turbulence, is a highly localized process. By contrast, in the study of Teixeira [2011b], the value found for c was 0.24, which is considerably smaller. If $\phi(z)$ was not included in (15), this would be approximately the value of c that would minimize the RMSE for the present data sets. However, as was seen above, $\phi(z)$ encapsulates important physics in the problem (practically all statistical measures are improved when it is included, as will be seen), so $c = 0.64$ will be adopted henceforth.

[32] Before more detailed comparisons with the WAVES and SWADE data sets are presented, it is worthwhile exploring the variation of the dissipation rate with the turbulent Langmuir number. Figure 2 shows $\varepsilon \kappa |z| / u_*^3$, as given by (18), as a function of La_t for $k_w |z| = 1$. In Figure 2a, results from the present model are displayed, showing its two asymptotic limits as $La_t \rightarrow \infty$ ($\varepsilon \kappa |z| / u_*^3 = 1$) and as $La_t \rightarrow 0$ ($\varepsilon \kappa |z| / u_*^3 = 0.82 La_t^{-2}$). Figure 2a bears a remarkable qualitative resemblance to Grant and Belcher [2009, Figure 4], showing the same kind of asymptotic behaviors. However, the dip in the curve at $La_t \approx 1$ does not occur. Such a dip would imply a decrease of the dissipation rate relative to its usual surface layer scaling for La_t in the range 0.4–2, which is not supported by the field data considered either here or in Teixeira [2011b]. Figure 2b shows a similar plot of ε using the model of Teixeira [2011b] (i.e., (18) with $\phi(z) = 1$) for the value of $c = 0.24$ resulting from the calibration of that model by Teixeira [2011b] against his data, and also for $c = 0.64$, as used here. It is clear that the asymptotic behavior of the model of Teixeira [2011b] is not in accordance with the scaling of Grant and Belcher [2009], overestimating the dissipation rate for low La_t . Nevertheless, over the range of La_t displayed by the data used by Teixeira [2011b] (0.3–0.8) the departure from the present model is slight when $c = 0.24$ is used, which explains why Teixeira [2011b] was able to obtain a good fit to the data. When $c = 0.64$ is used, however, as assumed in the present improved model, the overestimation produced by the model of Teixeira

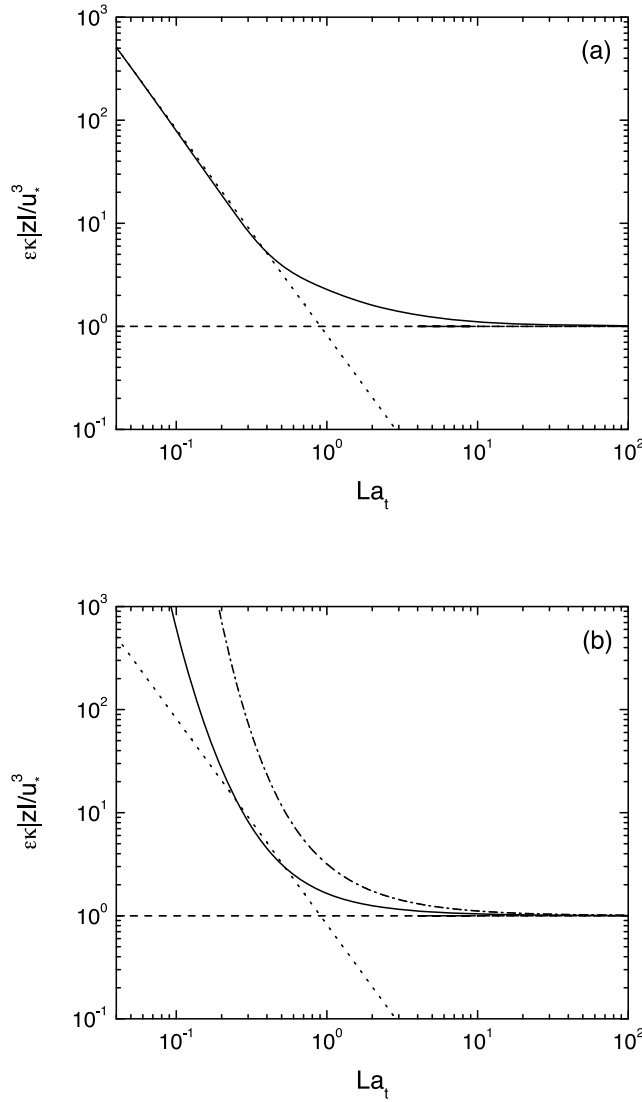


Figure 2. Normalized dissipation rate as a function of La_t for $k_w|z| = 1$. Dashed lines: $\epsilon\kappa|z|/u_*^3 = 1$, dotted lines: $\epsilon\kappa|z|/u_*^3 = 0.82La_t^{-2}$. (a) Solid line: present model (18) (with $c = 0.64$). (b) Model of Teixeira [2011b] ((18) with $\phi(z) = 1$) for $c = 0.24$ (solid line) and $c = 0.64$ (dash-dotted line).

[2011b] is much more pronounced. This is a consequence of erroneously assuming that the mean velocity profile in the wind-induced current is not changed by the presence of surface waves. An indication that this aspect has been adequately corrected in the present model is the fact that the asymptotic behavior in Figure 2a for low La_t is now consistent with that of Grant and Belcher [2009].

[33] The main subject of this section is now addressed. Figure 3 shows comparisons between $\log(\epsilon')$ calculated from various models and from the WAVES and SWADE observations. In Figure 3a, the theoretical values are given by the usual surface layer scaling, which when expressed in terms of ϵ' becomes:

$$\epsilon' = \frac{\epsilon H_s}{F} = \frac{1}{\alpha\kappa(z/H_s)}. \quad (28)$$

In Figure 3b, on the other hand, the theoretical values are given by the model of Craig and Banner [1994], more specifically using the uniformly valid approximation derived by Soloviev and Lukas [2003]:

$$\frac{\epsilon H_s}{F} = \frac{1}{\alpha\kappa(z/H_s + z_0/H_s)} \left[1 + 94.8 \left(\frac{z/H_s + z_0/H_s}{z_0/H_s} \right)^{-2.4} \right]. \quad (29)$$

It will be assumed that $z_0/H_s = 0.6$, which is supported by various authors [Terray et al., 1996; Soloviev and Lukas, 2003; Gerbi et al., 2009]. In Figure 3c the theoretical values of the dissipation rate are obtained from the model of Terray et al. [1996]:

$$\frac{\epsilon H_s}{F} = 0.3 \left(\frac{z}{H_s} \right)^{-2}. \quad (30)$$

In Figure 3d the dissipation rate is calculated from the model of Teixeira [2011b] (i.e., (15) with $\phi(z) = 1$ and $c = 0.24$). Finally, in Figure 3e the dissipation rate is calculated from (15) (with $c = 0.64$). All input parameters are taken from Terray et al. [1996, Tables 1 and 2] and Drennan et al. [1996, Table 1], and $\alpha = 100$ is always assumed.

[34] In Figure 3 it can be seen that the surface layer scaling (28) underestimates the dissipation rate in both the WAVES (open symbols) and SWADE (filled symbols) data sets. For the theory of Craig and Banner [1994], the underestimation still exists, but occurs mainly for the SWADE data set. The theory of Terray et al. [1996] fits quite well the WAVES data set (for which it was developed), but somewhat underestimates the SWADE data set. The model of Teixeira [2011b] corrects the underestimation of the SWADE data set but, on the other hand, overestimates some of its data points. The present model, (15), is the one that fits best both data, being able to correct the underestimation of the SWADE data set, while introducing no overestimation. There are some systematic differences in the agreement between the various theoretical predictions and measurements derived either from the horizontal or from the vertical velocity spectra (circles and triangles, respectively). These differences will be analyzed next.

[35] A better quantitative appraisal of the behavior of each model is obtained if the statistics defined above in (22), (24) and (25) are calculated for $\log(\epsilon')$. This is done in Table 1, where a clear improvement on the models of surface layer scaling, Craig and Banner [1994] and Terray et al. [1996], is obtained using the present model concerning all of the statistics considered. An improvement of the present model relative to the model of Teixeira [2011b] does not occur for all statistics, but is clearly verified for the RMSE.

[36] It is interesting to note that, in Table 1, for all theoretical predictions, the correlation is always lower and the RMSE larger for data derived from the vertical velocity spectrum (ϵ_w) than for data derived from the horizontal velocity spectrum (ϵ_u). Additionally, the values of both a and b are higher in the former case. This suggests that there is some slight systematic error in the procedure used to obtain the dissipation rate by each method, or in the underlying assumptions. For that reason, further statistics will carry on being calculated for ϵ_u or ϵ_w separately.

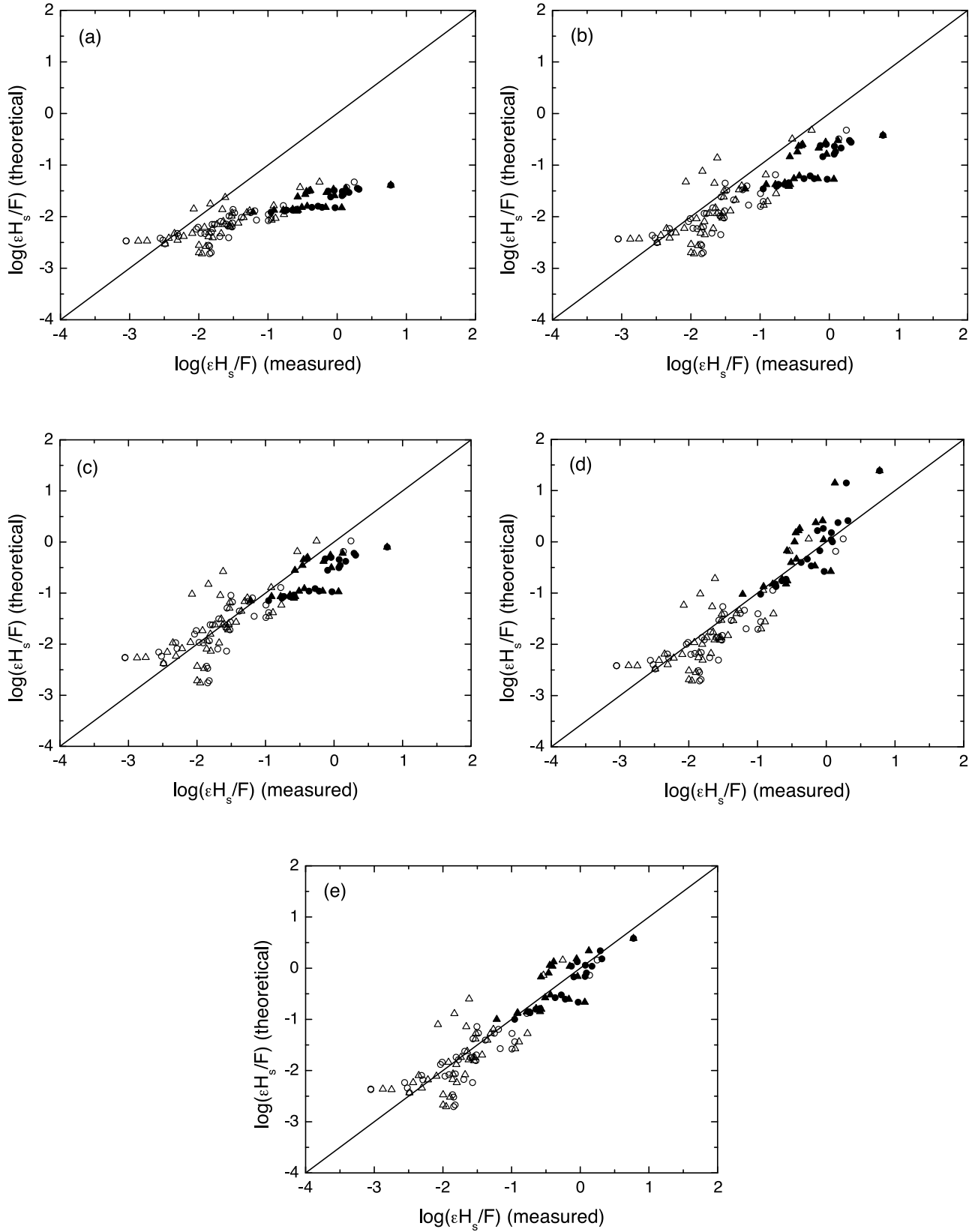


Figure 3. Comparison between measured and predicted logarithm of the normalized dissipation rate. Open symbols: WAVES data set, filled symbols: SWADE data set. Circles: dissipation estimated from horizontal velocity spectrum, triangles: dissipation estimated from vertical velocity spectrum. (a) Surface layer scaling. (b) Model of *Craig and Banner* [1994]. (c) Model of *Terray et al.* [1996]. (d) Model of *Teixeira* [2011b]. (e) Present model.

Table 1. Statistics of the Comparison Between Measured and Predicted Values of the Logarithm of the Normalized Dissipation Rate^a

WAVES+SWADE	Wall Layer		Craig and Banner [1994]		Terray <i>et al.</i> [1996]		Teixeira [2011b]		Present Model	
	ϵ_u	ϵ_w	ϵ_u	ϵ_w	ϵ_u	ϵ_w	ϵ_u	ϵ_w	ϵ_u	ϵ_w
R	0.910	0.840	0.924	0.846	0.910	0.840	0.937	0.904	0.941	0.892
b	0.352	0.371	0.663	0.692	0.704	0.741	1.040	1.128	0.909	0.972
$\log a$	-1.609	-1.536	-0.854	-0.721	-0.538	-0.390	-0.077	0.160	-0.228	-0.031
RMSE	1.061	0.925	0.614	0.547	0.448	0.444	0.379	0.443	0.336	0.399

^a R is the correlation coefficient, a and b are parameters of the linear fit (27) and RMSE is the root-mean square error. Measured values of $\log(\epsilon')$ are from the WAVES and SWADE data sets and theoretical values are predicted by various models (first line). ϵ_u and ϵ_w (second line) refer to dissipation rate values derived from measurements of the horizontal and vertical velocity spectra, respectively.

[37] Tables 2 and 3 show statistics similar to those contained in Table 1, with the difference that they are calculated separately for the WAVES and SWADE data sets. In Table 2, it can be seen that the present model manages to predict the WAVES data better than all other models, even that of *Terray et al.* [1996] (which was developed for this data set). The correlation values are higher for the present model, the values of b are closer to 1, the values of $\log a$ differ less from zero, and the RMSE is smaller than in all other models, including that of *Terray et al.* [1996]. This improvement is not as expressive, and does not occur for all statistics, using the model of *Teixeira* [2011b], which emphasizes the importance of the modifications introduced in the present study (these subtle differences were not obvious in Figure 3).

[38] For the SWADE data set, Table 3 shows that the present model is, without doubt, the one that presents the best performance, with considerably higher correlation coefficients, lower RMSE, and values of a and b closer to 1. The model of *Teixeira* [2011b] also provides a substantial improvement in the statistics, although globally not as large as the present model. For these data, the difference between the correlation coefficients of ϵ_u and ϵ_w is even larger than in the WAVES data set, however, in contrast, the value of b is higher for ϵ_u than for ϵ_w .

[39] Clearly, the improvement in the prediction of the SWADE data set must be related to some specific physical process that is captured by the present model. As noted by *Teixeira* [2011b], the average value of the turbulent Langmuir number is considerably lower in the SWADE data set ($La_t = 0.478$) than in the WAVES data set ($La_t = 0.694$). According to (17) and Figure 2, the dissipation rate increases as La_t decreases, which may explain why the present model corrects the underestimation of the SWADE data produced by the other models. On the other hand, the overestimation of some data points in the SWADE data set by the model of *Teixeira* [2011b] (see Figure 3d) is also consistent with Figure 2b, where it is shown that this model should

overestimate the dissipation rate at sufficiently low La_t . Not surprisingly, the values of La_t of these data points are among the lowest in the data set.

[40] *Teixeira* [2011b, Figure 1] presented the WAVE and SWADE data as a function of depth using different normalizations for ϵ and z . Although, from (17), it would be expected that the scaling adopted in that equation is the one that minimizes the data scatter, comparison between Figures 5 and 6 of *Drennan et al.* [1996] does not allow a clarification of which scaling variable works best: H_s or k_w . This problem is briefly addressed next.

[41] In Figure 4, the dissipation rate data from WAVES and SWADE are presented as a function of depth. The symbols have the same meaning as in Figure 3. Since the variation of the logarithm of the dissipation as a function of the logarithm of depth is reasonably linear, straight lines are fitted to these variations using F and H_s as scaling variables in Figure 4a and F and k_w instead in Figure 4b. The solid lines in Figures 4a and 4b correspond to linear fits of the variation of the logarithm of dimensionless dissipation versus the logarithm of dimensionless depth, whose parameters are shown in Table 4. The dashed lines correspond to the model of *Terray et al.* [1996] (in Figure 4a) and to the model of *Drennan et al.* [1996] (in Figure 4b). The latter can be expressed as:

$$\frac{\epsilon}{k_w F} = 0.1(k_w |z|)^{-2}. \quad (31)$$

In Table 4 it can be seen that the correlation coefficient is always larger, and the RMSE is smaller, for the scaling using k_w than for that using H_s . This suggests that the dimensionless depth $k_w |z|$ and dissipation rate $\epsilon/(k_w F)$ scalings, suggested by (17), are indeed the most appropriate in the problem.

3.2. Comparisons With Other Data Sets

[42] Results from the present model will now be compared with data from more recent sources. In the literature,

Table 2. Same as Table 1, but Including Data Only From the WAVES Data Set

WAVES	Wall Layer		Craig and Banner [1994]		Terray <i>et al.</i> [1996]		Teixeira [2011b]		Present Model	
	ϵ_u	ϵ_w	ϵ_u	ϵ_w	ϵ_u	ϵ_w	ϵ_u	ϵ_w	ϵ_u	ϵ_w
R	0.818	0.739	0.841	0.736	0.818	0.739	0.851	0.755	0.844	0.756
b	0.363	0.422	0.659	0.752	0.726	0.845	0.755	0.863	0.772	0.890
$\log a$	-1.587	-1.442	-0.856	-0.613	-0.493	-0.203	-0.615	-0.343	-0.491	-0.120
RMSE	0.706	0.601	0.469	0.450	0.394	0.438	0.414	0.436	0.383	0.431

Table 3. Same as Table 1, but Including Data Only From the SWADE Data Set

SWADE	Wall Layer		Craig and Banner [1994]		Terray <i>et al.</i> [1996]		Teixeira [2011b]		Present Model	
	ϵ_u	ϵ_w	ϵ_u	ϵ_w	ϵ_u	ϵ_w	ϵ_u	ϵ_w	ϵ_u	ϵ_w
R	0.892	0.657	0.890	0.650	0.892	0.657	0.922	0.803	0.928	0.732
b	0.369	0.283	0.746	0.566	0.892	0.566	1.383	1.251	0.994	0.815
$\log a$	-1.615	-1.580	-0.846	-0.779	-0.548	-0.480	0.112	0.311	-0.142	-0.030
RMSE	1.522	1.356	0.822	0.701	0.537	0.456	0.303	0.456	0.223	0.327

measurements of the dissipation rate are generally presented with much fewer details, concerning the wavefield and turbulence in the OBL, than in *Terray et al.* [1996] or *Drennan et al.* [1996]. Often, a typical value, or at most a histogram of the distribution of u_* / c_w or $k_w H_s$ is all that is provided for a whole set of measurements. That is the case in the studies that will be considered next. So, a typical value for these parameters is deduced from these studies in the most objective way possible. In all of these studies, the dissipation rate is presented as a function of depth, and both quantities are normalized using H_s and F . For that reason, the same scaling will be employed here.

[43] *Burchard* [2001] used two-equation turbulence models to simulate the behavior of various quantities beneath breaking surface waves, one of them being the dissipation rate. He tested the performance of the models using data from *Terray et al.* [1996], *Drennan et al.* [1996], and *Anis and Moum* [1995]. Although the first two sources of data overlap with those used in the previous section, they were normalized using an F calculated explicitly from its wave-age-dependent definition instead of using the parameterization expressed by (14). These data, as extracted from *Burchard* [2001, Figure 7], are reproduced in Figure 5a as the symbols. In that figure the dotted line corresponds to surface layer scaling (28), the dashed line corresponds to the model of *Terray et al.* [1996] (30), the dash-dotted line corresponds to the model of *Craig and Banner* [1994] (29), the thin solid line corresponds to the model of *Teixeira* [2011b] and the thick solid line corresponds to the present model (15). In *Terray et al.* [1996, Table 1], the average values of the parameters required in (15) are $u_* / c_w = 0.00573$ and $k_w H_s = 0.308$, and in *Drennan et al.* [1996, Table 1] those averages are instead $u_* / c_w = 0.00184$ and $k_w H_s = 0.254$. In the study of *Anis and Moum* [1995], the average values of the same parameters are $u_* / c_w = 0.00211$ and $k_w H_s = 0.268$. If these values are averaged (with equal weight) the global averages thus obtained are $u_* / c_w = 0.00323$ and $k_w H_s = 0.277$ (corresponding to $La_t = 0.580$). These values were employed both in the model of *Teixeira* [2011b] and in the present model.

[44] Looking at Figure 5a it can be seen that all models apart from the present one and that of *Teixeira* [2011b] underestimate the dissipation, with this underestimation being pronounced for the surface layer scaling, moderate for the model of *Craig and Banner* [1994] and relatively slight for the model of *Terray et al.* [1996]. It may be concluded that the present model is equally effective in predicting the dissipation rate whether F is parameterized using (14), or calculated using the presumably more accurate method developed by *Terray et al.* [1996]. This is a good indication that the value $\alpha = 100$ used in (14) and supported by various

authors [*Craig and Banner*, 1994; *Burchard*, 2001; *Kantha and Clayson*, 2004; *Stips et al.*, 2005] is adequate.

[45] More recently, *Gerbi et al.* [2009] carried out observations of turbulence in the OBL, obtaining new data for the

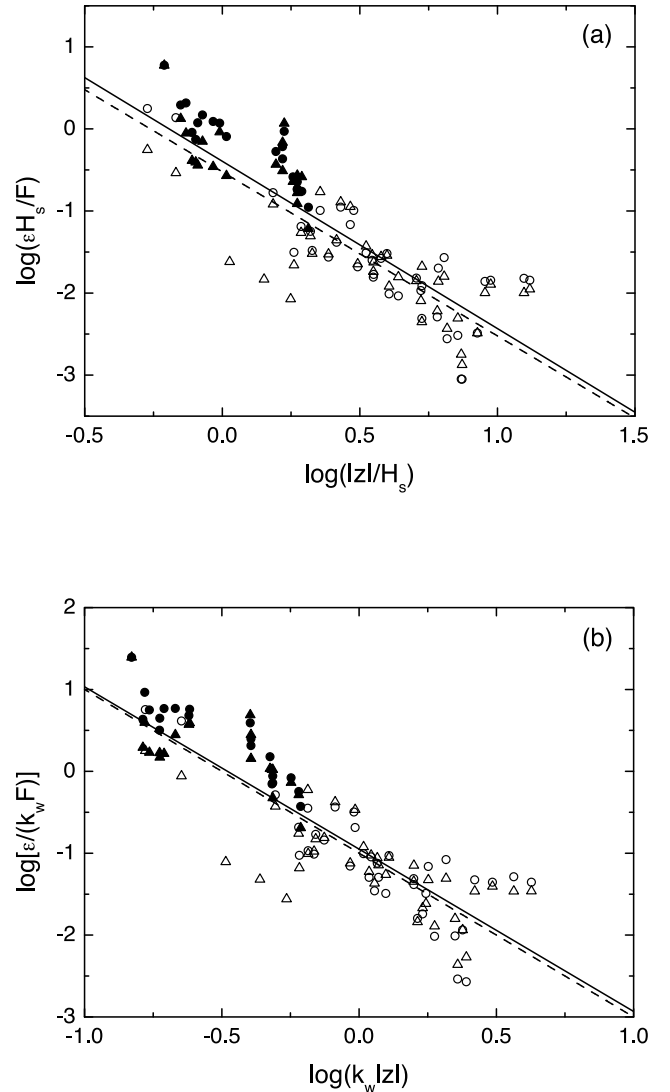


Figure 4. Logarithm of normalized dissipation rate as a function of logarithm of normalized depth for the WAVES and SWADE data sets. Meaning of symbols as in Figure 3. (a) Dissipation and depth normalized using H_s and F . Solid line: linear fit to data, dashed line: model of *Terray et al.* [1996]. (b) Dissipation and depth normalized using k_w and F . Solid line: linear fit to data, dashed line: model of *Drennan et al.* [1996].

Table 4. Statistics of a Linear Fit Between the Logarithm of the Dissipation and the Logarithm of Depth^a

WAVES +SWADE	Scaling Using H_s		Scaling Using k_w	
	<i>Terray et al.</i> [1996]	Linear Fit	<i>Drennan et al.</i> [1996]	Linear Fit
R	0.859	0.859	0.880	0.880
b	-2	2.039	-2	-1.983
$\log a$	-0.523	-0.394	-1	-0.950
RMSE	0.435	0.420	0.410	0.407

^aThe parameters have the same meaning as in the previous tables and in (27), with the difference that they are applied to a linear relationship between the logarithm of dissipation and the logarithm of depth, as defined in Figures 4a and 4b, respectively. ‘Linear fit’ refers to the values that minimize the RMSE in each case.

dissipation rate beneath both wind waves and swell. Swell corresponds to waves that may be propagating in a different direction from that of the surface wind stress. In those circumstances dU/dz and dU_s/dz may not be aligned, and (15) will be expected to overestimate the dissipation rate. This is consistent with the conclusion of *Cox* [1997] that the growth of Langmuir circulations is reduced by misalignment between the shear flow and the Stokes drift that generate them.

[46] For these reasons, only the dissipation data for the wind waves case, contained in *Gerbi et al.* [2009, Figure 9a], will be considered next. These data were extracted and are presented in Figure 5b as the symbols. The lines have the same meaning as in Figure 5a. The dissipation data in *Gerbi et al.* [2009, Figure 9a] use $\alpha = 168$ in the definition of F according to (14) in order to obtain a better fit using the

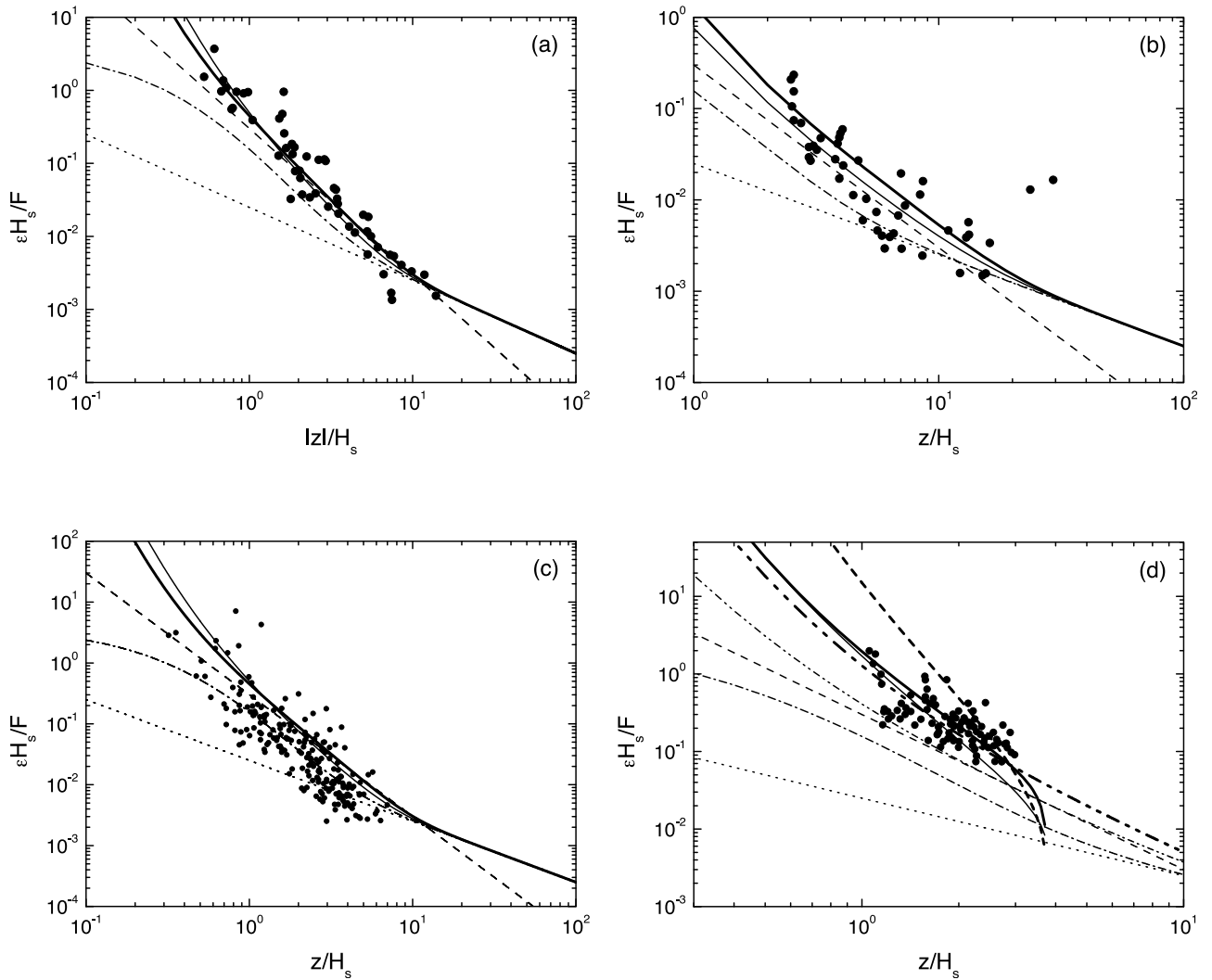


Figure 5. Normalized dissipation rate as a function of normalized depth from various recent sources compared with theoretical models. Dotted lines: surface layer scaling, thin dashed lines: model of *Terray et al.* [1996], dash-dotted lines: model of *Craig and Banner* [1994], thin solid lines: model of *Teixeira* [2011b], thick solid lines: present model. (a) Data from *Burchard* [2001]. (b) Data from *Gerbi et al.* [2009]. (c) Data from *Jones and Monismith* [2008]. (d) Data from *Feddersen et al.* [2007]. Dash-dot-dotted lines: deep-water approximation, solid lines: finite water depth, thick dashed line: no shallow-water effects in $\phi(z)$.

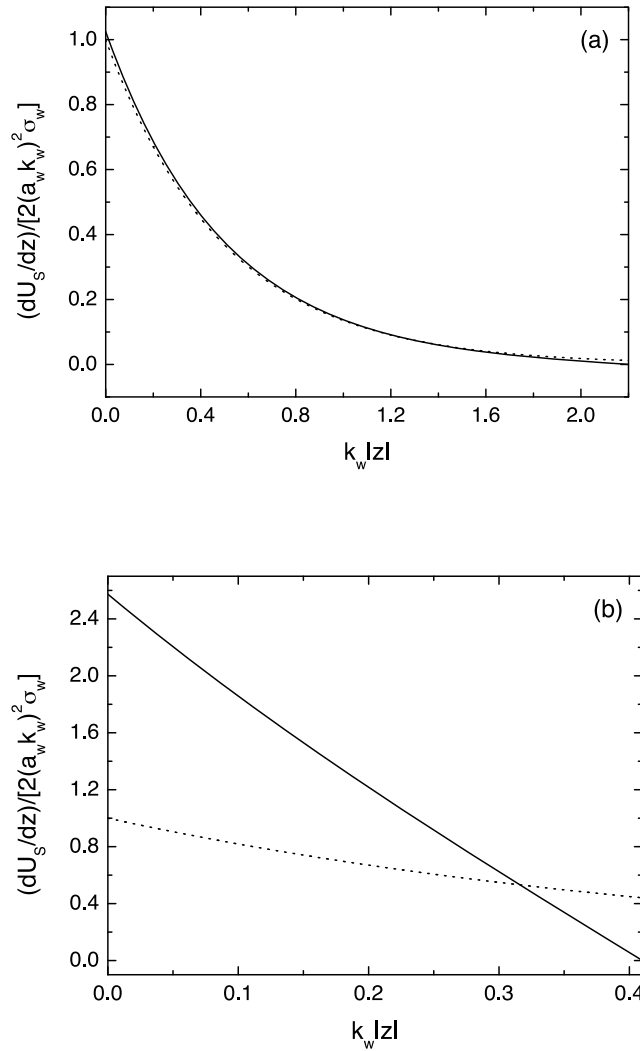


Figure 6. Profile of the normalized strain rate of the Stokes drift for a monochromatic surface wave as a function of normalized depth from linear wave theory, for arbitrary water depth (solid lines) and in the deep-water approximation (dotted lines). (a) Shown is $k_w h = 2.2$, as in *Jones and Monismith* [2008], and (b) $k_w h = 0.41$, as in *Feddersen et al.* [2007].

model of *Terray et al.* [1996] (30). Since here the value $\alpha = 100$ is always used, the corresponding data plotted in Figure 5b have been multiplied by a factor of 1.68. From *Gerbi et al.* [2009, Figure 5a], the dominant significant wave height of wind waves was estimated as $H_s = 0.6$ m. From *Gerbi et al.* [2009, Figure 8], on the other hand, the dominant angular frequency of wind waves was estimated as $\sigma_w = 1.4 \text{ rad s}^{-1}$, which leads to $k_w = 0.2 \text{ m}^{-1}$ using the linear dispersion relation of surface gravity waves. This yields $k_w H_s = 0.12$. Finally, from *Gerbi et al.* [2009, Figure 5c], the dominant wave age was estimated as 30, which, via continuity of the surface stress at the air-water interface gives $u_*/c_w = 0.0012$. Both of these values (which correspond to $La_t = 0.816$) were used in the present model.

[47] In Figure 5b it can be seen that, once again, the present model and the model of *Teixeira* [2011b] provide the best fit to the data, followed by the models of *Terray et al.*

[1996], *Craig and Banner* [1994] and surface layer scaling. The model of *Teixeira* [2011b] is perhaps slightly better at larger depths (if the outlying points are ignored) and the present model is perhaps slightly better near the surface, but differences are not very significant. The fact that good agreement is possible without having to change the value of the constant α confirms that F may not be a key quantity determining the dissipation rate. The need of *Gerbi et al.* [2009] to change α in order to obtain good agreement with the model of *Terray et al.* [1996] may be an artifact of the dependence of that model on that parameter. This aspect will be further addressed below.

[48] *Jones and Monismith* [2008] recently investigated the effect of whitecaps on the vertical structure of turbulence in a relatively shallow estuary. They obtained new dissipation rate measurements, which are presented in their Figure 12. The data in *Jones and Monismith* [2008, Figure 12a] are reproduced in Figure 5c as the symbols. The lines have the same meaning as in Figure 5b. The parameters of the present model have been obtained in the following way. The dominant significant wave height was estimated from *Jones and Monismith* [2008, Figure 6a] as $H_s = 0.26$ m. The dominant wave number could not be inferred from Figure 6b of the same study, because what is presented is the average wave period, which is different from the peak wave period [see *Jones and Monismith*, 2007]. The peak wave number in the measurements of *Jones and Monismith* [2008] is in fact about $k_w = 1.05 \text{ m}^{-1}$ (N. L. Jones, personal communication, 2010), so the value of the wave slope employed in the present model is $k_w H_s = 0.273$. From *Jones and Monismith* [2008, Figure 6c], the dominant wave age is estimated as 11, which gives $u_*/c_w = 0.00315$. These two values yield $La_t = 0.581$.

[49] In Figure 5c it can be seen that the present model, as well as the model of *Teixeira* [2011b], somewhat overestimate the dissipation rate data, while the model of *Terray et al.* [1996] is of comparable accuracy, and both the model of *Craig and Banner* [1994] and especially surface layer scaling, underestimate the data. Nevertheless, the present model and the model of *Teixeira* [2011b] reproduce better the trend of the data with depth at small $|z|/H_s$, whereas all other models underestimate the dissipation rate more severely at these depths.

[50] It should be noted that the dissipation estimates from the present model were calculated using the deep-water formula (15). It might appear that the conditions are too shallow for this, but *Jones and Monismith* [2008] refer that, for the peak of the wave spectrum, $k_w h = 2.2$. Since $\tanh(k_w h) = 0.976$, this effect is expected to be almost insignificant, and calculations of the dissipation rate using the arbitrary depth formula (20) confirmed this. For that reason, (15) has been used, as in the previous cases (see further discussion below).

[51] The reason for the overestimation of the dissipation rate by the present model may be related with the fact, mentioned in *Jones and Monismith* [2008, p. 1567] that, due to wave refraction by the bathymetry, “the wave direction was predominantly toward the northeast for a range of wind directions.” In these circumstances, the Stokes drift of the waves and the surface stress (and the corresponding current shear) are generally not aligned, which is at odds with the assumptions of the present model. It would be interesting to

extend the model to overcome this limitation, but that is beyond the scope of the present paper.

[52] The final field study to be mentioned is that carried out by *Feddersen et al.* [2007], addressing the vertical structure of dissipation in the nearshore. The measurements of the dissipation rate carried out by *Feddersen et al.* [2007] are presented in their Figure 11b. In order to fit the model of *Terray et al.* [1996] to their data, *Feddersen et al.* [2007] again changed the value of the constant in the definition of F (14) to $\alpha = 250$, which does not seem a very satisfactory approach. The data of *Feddersen et al.* [2007] are reproduced in Figure 5d as the symbols, albeit multiplied by a factor of 2.5, which corresponds to assuming $\alpha = 100$, as usual. The lines have the same meaning as in Figure 5c, except that the solid lines now correspond to the dissipation rate using the formulas valid for arbitrary water depth (20), whereas the dash-dot-dotted lines use the deep-water formulas (15). The thick dashed line corresponds to a model that uses (20), but where $\phi(z)$ does not take into account shallow-water effects (16).

[53] *Feddersen et al.* [2007, p. 1766] mention that the peak period of the surface waves is between 9 and 10 s. Taking an average value of 9.5 s and using the linear dispersion relation, $\sigma_w = [gk_w \tanh(k_w h)]^{1/2}$, noting also that typically $k_w h = 0.41$ at the measurement location [*Feddersen et al.*, 2007], one gets a dominant wave number $k_w = 0.115 \text{ m}^{-1}$. From *Feddersen et al.* [2007, Figure 3b], the dominant significant wave height is estimated as $H_s = 1 \text{ m}$. This gives $k_w H_s = 0.11$, a value used in the present model. Secondly, from *Feddersen et al.* [2007, Figure 3d], the friction velocity is estimated as $u_* = 0.01 \text{ ms}^{-1}$. Since $c_w = 5.76 \text{ ms}^{-1}$, this yields $u_*/c_w = 0.00174$, a value also adopted here. This corresponds to $La_t = 0.549$.

[54] Figure 5d shows that all models except the present model including full shallow water effects underestimate the measurements of the dissipation rate. While the present model using the deep-water approximation produces a relatively modest underestimation, the same model including shallow-water effects in (20), but excluding them in the definition of $\phi(z)$ considerably overestimates the data. The model of *Teixeira* [2011b], on the other hand, is as accurate as the present one when shallow water effects are taken into account, except at larger depths. The same model using the deep-water approximation underestimates much more severely the data. This suggests that only the complete model is physically consistent, and that the shape of the Stokes drift profile, rather than any change in the scaling of F , crucially determines the dissipation enhancement in the present case.

[55] The mechanism through which this enhancement arises, which is inaccessible to any other of the theoretical models under consideration except that of *Teixeira* [2011b], is illustrated in Figure 6. Figure 6a shows the difference between normalized dU_s/dz as a function of depth for $k_w h = 2.2$ (the case considered by *Jones and Monismith* [2008]), using the deep-water approximation (5) and for arbitrary water depth (19). Figure 6b shows the same quantities for $k_w h = 0.41$, i.e., the case considered by *Feddersen et al.* [2007]. It can be seen that, while in the first case the differences between the Stokes drift strain rate in the two approximations are minimal, they are very large in the second case. In this last case, the Stokes drift strain rate is much

higher, by a factor of more than 2 near the surface, than the strain rate predicted with the deep-water approximation. This increase in the strain rate is responsible, in the present model, for the enhancement of the dissipation rate that is necessary to match the data.

[56] It is also interesting to note that the dissipation rate is slightly underestimated by the present model, even taking shallow-water effects into account, at the largest values of $|z|/H_s$ reached by the data. This is probably due to the neglect of the bottom boundary layer, since the data for which this underestimation occurs are relatively close to the ocean bottom.

4. Concluding Remarks

[57] A theoretical model for estimating the TKE dissipation rate in the surface layer of the OBL, based on RDT arguments, was described and tested in the present study. The model improves that of *Teixeira* [2011b] by taking into account the partition of the shear stress into shear-induced and wave-induced components, an important aspect of the OBL that leads to substantial weakening of the mean shear rate near the surface. The model aims to provide an alternative explanation for the very high values of dissipation rate observed in various existing data sets. It is assumed in the model that, at equilibrium, when the dominant values of the dissipation rate are presumably attained, production of TKE by the shear of the mean Eulerian flow and by the Stokes drift gradient of surface waves approximately balance dissipation. In this framework, the dissipation enhancement arises from a saturated state of the same instability mechanism that is accepted to be the source of Langmuir circulations in the OBL, which is shown to be associated with a vigorous amplification of the turbulent shear stress. Like all models based on RDT, the present model assumes that this amplification proceeds until it is halted by nonlinear processes at a time of the order the eddy turn-over time of the turbulence. Since this turbulence is most probably generated initially by wave breaking, the eddy turn-over time in the OBL is scaled as $T_L \sim (k_w u_*)^{-1}$.

[58] The model predicts that the dissipation rate, when normalized in conventional ways, is a function not only of a dimensionless depth, but also of dimensionless parameters u_*/c_w and $k_w H_s$, related with the wave age and wave slope, respectively. When the dissipation rate is normalized using k_w or z instead of H_s , these two controlling parameters reduce to one, the turbulent Langmuir number La_t . This result emphasizes the connection between dissipation enhancement and Langmuir turbulence [*McWilliams et al.*, 1997]. According to the present model, the depth over which the dissipation rate is enhanced scales like k_w^{-1} , not H_s .

[59] The model was first calibrated (the constant of proportionality in the relationship $T_L = c(k_w u_*)^{-1}$ was estimated as $c = 0.64$) using the WAVES and SWADE data sets [*Terray et al.*, 1996; *Drennan et al.*, 1996]. Its performance was then assessed by first calculating various statistics of its prediction of the logarithm of the dissipation rate in the same data sets. The correlation coefficient, linear regression parameters and RMSE were shown to be improved by the present model relative to surface layer scaling, the model of *Craig and Banner* [1994], the model of *Terray et al.* [1996]

and the model of Teixeira [2011b]. The new model was then tested against dissipation data from Burchard [2001], Feddersen et al. [2007], Jones and Monismith [2008] and Gerbi et al. [2009]. The agreement of the present model with these data sets is clearly better than that of previous models, except for the data of Jones and Monismith [2008], where considerable wave refraction effects are thought to be present. In particular, it is unnecessary to change the constant in the expression for the energy flux F , α , to fit the data, as, for example, Feddersen et al. [2007] and Gerbi et al. [2009] had done. In fact, F is not an important parameter in the present model.

[60] Both when an improvement on previous models was obtained and in the cases where the model failed, a clear physical interpretation could be ascribed to this behavior. Hence, for example, the data of Feddersen et al. [2007] could only be predicted adequately using a formula for the dissipation rate that fully takes into account the effect of finite water depth, because this effect increases the strain rate of the Stokes drift by a factor of 2 or more. This increase is thought to be responsible for part of the observed enhancement of the dissipation rate in the data. Additionally, when the new model overestimates the dissipation rate in the observations of Jones and Monismith [2008], this overestimation is attributable to the fact that the Stokes drift of the waves may not have been aligned with the surface shear, as is assumed in the model.

[61] The present model does not have the roughness length z_0 as an input parameter, and in that respect it circumvents the problem of relating this quantity to other quantities, like for example H_s . This is apparently an advantage over the model of Craig and Banner [1994], which is very sensitive to the prescription of this quantity.

[62] The friction velocity used in the present model implicitly assumes a simple viscous coupling between the ABL and the OBL, as has been done by numerous previous authors [Terray et al., 1996; Drennan et al., 1996; Gerbi et al., 2009]. Since this friction velocity exists before any amplification of the shear stress by the mechanism that is at the heart of the model has taken place (see (3) and (4)), it obviously provides an underestimate of the actual near-surface shear stress in the OBL when dissipation is enhanced. However, if this friction velocity is used instead as a measure of the mean shear (e.g., assuming a logarithmic mean velocity profile), it leads to an overestimation of the shear rate, since the shear stress is actually partitioned into a shear-induced and a wave-induced part, as was fully taken into account here. This partitioning is crucial not only for obtaining realistic estimates of the shear rate in the OBL, but also for improving the agreement of the model with observations, in particular avoiding the overestimation of the dissipation rate at low La_t produced by the model of Teixeira [2011b], and achieving an asymptotic behavior, as $La_t \rightarrow 0$, in agreement with Grant and Belcher [2009], namely $\epsilon \propto La_t^{-2}$.

[63] There are few reasons to doubt that the dissipation enhancement mechanism proposed here acts almost continuously in the OBL, since wind-forcing, turbulence and surface waves are ubiquitous there. It is left for future studies to understand how this mechanism fits together with competing ones.

[64] **Acknowledgments.** I am grateful to two anonymous referees, whose insightful comments have greatly helped to improve this paper. I acknowledge the financial support of the Portuguese Science Foundation (FCT) under projects PEst-OE/CTE/LA0019/2011-IDL and PTDC/CTE-ATM/122501/2010.

References

- Agrawal, Y. C., E. A. Terray, M. A. Donelan, P. A. Hwang, A. J. Williams III, W. M. Drennan, K. K. Kahma, and S. A. Kitaigorodskii (1992), Enhanced dissipation of kinetic energy beneath surface waves, *Nature*, **359**, 219–220.
- Anis, A., and J. N. Moum (1995), Surface wave-turbulence interactions: Scaling $\epsilon(z)$ near the sea surface, *J. Phys. Oceanogr.*, **25**, 2025–2045.
- Burchard, H. (2001), Simulating the wave-enhanced layer under breaking surface waves with two-equation turbulence models, *J. Phys. Oceanogr.*, **31**, 3133–3145.
- Cox, S. M. (1997), Onset of Langmuir circulation when shear flow and Stokes drift are not parallel, *Fluid Dyn. Res.*, **19**, 149–167.
- Craig, P. D., and M. L. Banner (1994), Modeling wave-enhanced turbulence in the ocean surface layer, *J. Phys. Oceanogr.*, **24**, 2546–2559.
- Csanady, G. T. (2004), *Air-Sea Interaction: Laws and Mechanisms*, Cambridge Univ. Press, Cambridge, U. K.
- Drennan, W. M., K. K. Kahma, E. A. Terray, M. A. Donelan, and S. A. Kitaigorodskii (1992), Observations of the enhancement of kinetic energy dissipation beneath breaking wind waves, in *Breaking Waves: IUTAM Symposium Sydney, Australia*, edited by M. L. Banner and R. H. J. Grimshaw, pp. 95–102, Springer, New York.
- Drennan, W. M., M. A. Donelan, E. A. Terray, and K. B. Katsaros (1996), Oceanic turbulence dissipation measurements in SWADE, *J. Phys. Oceanogr.*, **26**, 808–815.
- Feddersen, F., J. H. Trowbridge, and A. J. Williams III (2007), Vertical structure of dissipation in the nearshore, *J. Phys. Oceanogr.*, **37**, 1764–1777.
- Gerbi, G. P., J. H. Trowbridge, E. A. Terray, A. J. Plueddemann, and T. Kukulka (2009), Observations of turbulence in the ocean surface boundary layer: Energetics and transport, *J. Phys. Oceanogr.*, **39**, 1077–1096.
- Grant, A. L. M., and S. E. Belcher (2009), Characteristics of Langmuir turbulence in the ocean mixed layer, *J. Phys. Oceanogr.*, **39**, 1871–1887.
- Holton, J. R. (2004), *An Introduction to Dynamic Meteorology*, 4th ed., Elsevier, New York.
- Jones, N. L., and S. G. Monismith (2007), Measuring short-period wind waves in a tidally forced environment with a subsurface pressure gauge, *Limnol. Oceanogr. Methods*, **5**, 317–327.
- Jones, N. L., and S. G. Monismith (2008), The influence of whitecapping waves on the vertical structure of turbulence in a shallow estuarine embayment, *J. Phys. Oceanogr.*, **38**, 1563–1580.
- Kantha, L. H., and C. A. Clayson (2004), On the effect of surface gravity waves on mixing in the oceanic mixed layer, *Ocean Modell.*, **6**, 101–124.
- Kukulka, T., A. J. Plueddemann, J. H. Trowbridge, and P. P. Sullivan (2010), Rapid mixed layer deepening by the combination of Langmuir and shear instabilities: A case study, *J. Phys. Oceanogr.*, **40**, 2381–2400.
- Leibovich, S. (1983), The form and dynamics of Langmuir circulations, *Annu. Rev. Fluid Mech.*, **15**, 391–427.
- Li, M., C. Garret, and E. Skillingstad (2005), A regime diagram for classifying turbulent large eddies in the upper ocean, *Deep Sea Res., Part I*, **52**, 259–278.
- McWilliams, J. C., P. P. Sullivan, and C.-H. Moeng (1997), Langmuir turbulence in the ocean, *J. Fluid Mech.*, **334**, 1–30.
- Melville, W. K. (1996), The role of surface-wave breaking in air-sea interaction, *Annu. Rev. Fluid Mech.*, **28**, 279–321.
- Noh, Y., H. S. Min, and S. Raasch (2004), Large eddy simulation of the ocean mixed layer: the effects of wave breaking and Langmuir circulation, *J. Phys. Oceanogr.*, **34**, 720–735.
- Polton, J. A., and S. E. Belcher (2007), Langmuir turbulence and deeply penetrating jets in an unstratified mixed layer, *J. Geophys. Res.*, **112**, C09020, doi:10.1029/2007JC004205.
- Soloviev, A., and R. Lukas (2003), Observation of wave-enhanced turbulence in the near-surface layer of the ocean during TOGA COARE, *Deep Sea Res., Part I*, **50**, 371–395.
- Stips, A., H. Burchard, K. Bolding, H. Prandke, A. Simon, and A. Wüest (2005), Measurement and simulation of viscous dissipation in the wave affected surface layer, *Deep Sea Res., Part II*, **52**, 1133–1155.
- Sullivan, P. P., J. C. McWilliams, and W. K. Melville (2004), The oceanic boundary layer driven by wave breaking with stochastic variability. Part I. Direct numerical simulations, *J. Fluid. Mech.*, **507**, 143–174.

- Sullivan, P. P., J. C. McWilliams, and W. K. Melville (2007), Surface gravity wave effects in the oceanic boundary layer: large-eddy simulation with vortex force and stochastic breakers, *J. Fluid Mech.*, 593, 405–452.
- Teixeira, M. A. C. (2011a), A linear model for the structure of turbulence beneath surface water waves, *Ocean Modell.*, 36, 149–162.
- Teixeira, M. A. C. (2011b), On the connection between dissipation enhancement in the ocean surface layer and Langmuir circulations, *J. Phys. Oceanogr.*, 41, 2000–2007.
- Teixeira, M. A. C., and S. E. Belcher (2000), Dissipation of shear-free turbulence near boundaries. *J. Fluid Mech.*, 422, 167–191.
- Teixeira, M. A. C., and S. E. Belcher (2010), On the structure of Langmuir turbulence, *Ocean Modell.*, 31, 105–119.
- Terray, E. A., M. A. Donelan, Y. C. Agrawal, W. M. Drennan, K. K. Kahma, A. J. Williams III, P. A. Hwang, and S. A. Kitaigorodskii (1996), Estimates of kinetic energy dissipation under breaking waves, *J. Phys. Oceanogr.*, 26, 792–807.